Ceramics International 51 (2025) 8941–8954

Contents lists available at ScienceDirect

Ceramics International

journal homepage: www.elsevier.com/locate/ceramint

Upcycling municipal solid waste incineration bottom ash in clay-bonded bricks

Adeolu Adediran [a,*], Shaurin Maher Kikky [a], Suman Kumar Adhikary [a], Vilma Ducman [b], Priyadharshini Perumal [a]

[a] Fibre and Particle Engineering Research Unit, University of Oulu, Pentti Kaiteran Katu 1, 90014, Oulu, Finland
[b] Slovenian National Building and Civil Engineering Institute (ZAG), Dimičeva 12, 1000, Ljubljana, Slovenia

ARTICLE INFO

Handling Editor: Dr P. Vincenzini

Keywords:
Bottom ash
Kaolinite clay
Illite clay
Bricks
Circular economy
Durability

ABSTRACT

There is an increasing concern about the management of municipal solid waste incineration bottom ash (BA), of which approximately 300,000 tons are generated annually in Finland. As an alternative to the landfilling of this waste, which is the most common practice in the industry, this study investigates the feasibility of upcycling BA for clay brick production. Here, kaolinitic and illitic clays were selected as the precursors. Kaolinitic or illitic clays containing 10, 20, and 30 wt% BA and their counterparts without BA were fired at 1000 °C. The materials and prepared bricks were characterized using X-ray diffraction, thermogravimetry, scanning electron microscopy coupled with energy-dispersive X-ray spectroscopy, mass loss, visual appearance, linear shrinkage, water absorption, apparent density, compressive strength, freeze–thaw, and leaching tests. The experimental results show that the incorporation of BA as an admixture positively influenced the properties of illitic clay-based bricks, which exhibited a reduction in cracks, mass loss, and water absorption while having higher apparent density, compressive strength, and residual strength than kaolinitic clay-based bricks. This is mainly ascribed to the difference in their sintering behavior and chemical and mineralogical composition; more notably, it is ascribed to the higher content of alkali oxides (K_2O and Na_2O) in the illitic clay than in the kaolinitic clay. The water absorption of the bricks varied from 4 % to 25 %, and the compressive strength varied from 12 to 19 MPa depending on the BA content and clay type. Nevertheless, the compressive strength of all bricks satisfied the ASTM C62 standard for bricks subjected to negligible weathering, and the residual strength of some samples after exposure to 50 freeze–thaw cycles demonstrated their resistance to severe weathering. The dual effects of sintering and BA addition resulted in more stable crystalline phases and a densified microstructure. Moreover, the heavy metals in BA were encapsulated in kaolinitic and illitic clay bricks and satisfied EU regulations for inert and nonhazardous materials.

1. Introduction

Owing to the growing population and increasing human needs, municipal solid waste (MSW) is increasing tremendously. The World Bank estimated 2.01 billion tons of MSW in 2016 and predicted that it could increase to 3.4 billion tons by 2050 [1]. In most developed countries, most of the generated MSW is incinerated to generate energy for use. The incineration method is gaining popularity worldwide due to its 70%–90 % waste volume reduction efficiency and energy recovery from MSW, thus enabling waste-to-energy conversion [2,3]. It was reported that the waste-to-energy market is growing by 7.4 % annually, suggesting the production of enormous amounts of municipal solid waste incineration (MSWI) ash [1]. During the MSWI process, bottom ash (BA), fly ash (FA), and air pollution ash are some of the produced byproducts, among which BA constitutes a large proportion of the ashes produced [1]. In Finland alone, approximately 300,000 tons of BA are produced annually. Most of the MSWI ashes are landfilled owing to the large volume in which they are produced. In the future, the cost of landfilling is expected to increase, and the number of landfills will remain the same, necessitating the need to find a sustainable alternative to landfilling. Several pathways have been proposed and explored for these ashes, principal among them being their use as precursors for various applications. Some notable applications in which BA has been used include backfill and road subbase, aggregates, and cementitious

* Corresponding author.
E-mail address: adeolu.adediran@oulu.fi (A. Adediran).

https://doi.org/10.1016/j.ceramint.2024.12.324
Received 16 July 2024; Received in revised form 3 December 2024; Accepted 19 December 2024
Available online 20 December 2024

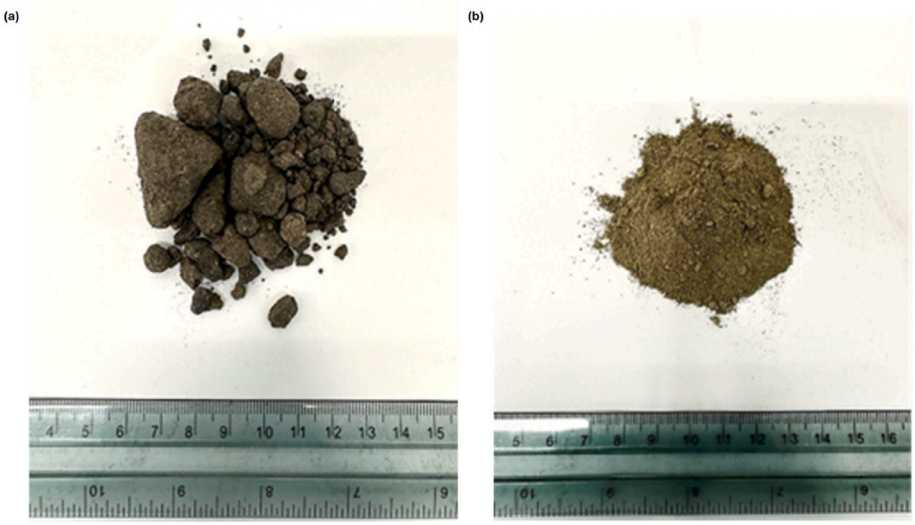

Fig. 1. London clay (a) as received and (b) after milling.

binders in construction applications [4–8]. However, the main concern is the safety caused by the source of this material and the presence of residual metallic elements in some ashes after the incineration process [9].

Recently, various approaches have been implemented in research and practice to stabilize heavy metal levels in MSWI ash samples, thereby limiting leaching levels and meeting legislative regulations. For instance, melting at high temperatures, thermal treatment, and sintering are reliable approaches to detoxicate MSWI ash samples, offering the benefit of minimal leaching of heavy metals [10,11]. Numerous studies have reported a dramatic reduction in heavy metal leaching from MSWI ash-based products via sintering techniques [12–14]. Zhang et al. [15] sintered MSWI ashes at 700°C-1000 °C and reported a decline in heavy metal leaching with increasing sintering temperature. In the mentioned study, the sintered ash completely immobilized the heavy metals, indicating that there were no environmental threats. Cheeseman et al. [16] developed lightweight aggregates from incinerated BA using a sintering process; a significant decrease in heavy metal leaching was reported in the sintered aggregates. A similar observation was reported by Bethanis et al. [17] where a significant reduction in heavy metal leaching was noticed in the sintered incinerated BA. Hence, the production of bricks with MSWI ash using a high-temperature sintering method is a potential approach for reusing MSWI ash.

Clay has been used for brick production since ancient times, and in recent years, the incorporation of solid waste into fired clay bricks or tiles has gained considerable interest. Researchers from across the world have used many waste materials in clay bricks, including sugarcane bagasse ashes [18], coal FA [19], marble powder [20], paper waste [21], and construction and demolition waste [22]. Several studies have shown that the technical performance of clay bricks is significantly influenced by the type and content of waste materials. Kazmi et al. [23] reported a 35 % and 34.4 % reduction in the compressive strength of clay bricks containing RHA and sugarcane bagasse ash, respectively. In another study, Rasool et al. [24] reported a 41 % decrease in the mechanical performance of clay bricks incorporating 15 % waste marble powder. In addition, the authors reported that adding MSWI ash decreased drying shrinkage by 15 % and total shrinkage by 24 %. Lin [25] used MSWI slag as a partial substitute for clay in brick production and reported that the compressive strength of bricks with 40 % MSWI slag content remained almost similar to that of normal clay bricks heated at 1000 °C. Kizinievič et al. [26] incorporated 15 % BA in clay brick and reported approximately 21 % decrease in the drying shrinkage. The compressive strength of the brick decreased with increasing BA dose, which can be attributed to the increase in porosity. This extensive literature review demonstrates the potential for the reuse of MSWI ash samples as a partial substitute for clay in brick production. It is also evident that the presence of heavy metals in these ashes is immobilized during high-temperature firing, presenting an opportunity for the reuse of solid waste materials in the construction industry while meeting the regulatory limits provided by legislation.

Recently, researchers have used MSWI ash samples for clay brick production, focusing on the mechanical performance, shrinkage, mass loss, water absorption, and heavy metal leaching of bricks. However, most of the studies have focused mainly on the use of MSWI FA in clay brick production, with limited research on clay-based bricks containing BA. One of the studies that used BA from a coal power plant in the ceramic sector found that in addition to the chemical composition, the pressure applied during forming, sintering temperature, and particle size play crucial roles in the development of mechanical properties [27]. The need to fire bricks at high temperatures (mainly above 1000 °C) is often considered a drawback in the manufacturing of bricks, particularly in terms of energy demand and production cost [28]. To reduce the firing temperature, some commercial ingredients containing Na_2O, K_2O, or MgO have been investigated as fluxing agents [29]. Firing at low temperatures with the aid of fluxing agents has been reported to have numerous advantages, such as a reduction in the release and concentration of emissions from the firing process, an increase in the formation of the glass phase, a decrease in porosity, and enhancement of the mechanical properties of bricks [28]. Interestingly, the BA used in this study contains high amounts of Na_2O, K_2O, and CaO, which can act as fluxing agents. It is postulated that mixing illitic or kaolinitic clay with BA will result in complementary advantages and improvements in the performance of clay bricks fired at low temperatures. Even though, there are few reports on the recycling of BA in clay bricks [26,27], a comprehensive experimental study on the compatibility of BA with different types of clay (kaolinitic and illitic) is lacking. Hence, the aim of this study was to investigate the properties of clay bricks made from different types of clay containing BA. The replacement of 10, 20, and 30 wt% clay with BA was investigated. The compositions of kaolinitic and illitic clays containing BA and their counterparts without BA were fired at 1000 °C. The phase compositions and microstructural evolutions were investigated using X-ray diffraction (XRD), thermogravimetry (TG), and scanning electron microscopy (SEM) coupled with energy-dispersive X-ray spectroscopy (EDS). The physical and mechanical properties of the clay bricks were assessed in terms of their visual appearance, compressive strength, mass loss, and linear shrinkage. The durability of the materials was assessed in terms of water absorption, apparent density, freeze–thaw, and leaching tests to better characterize the prepared bricks.

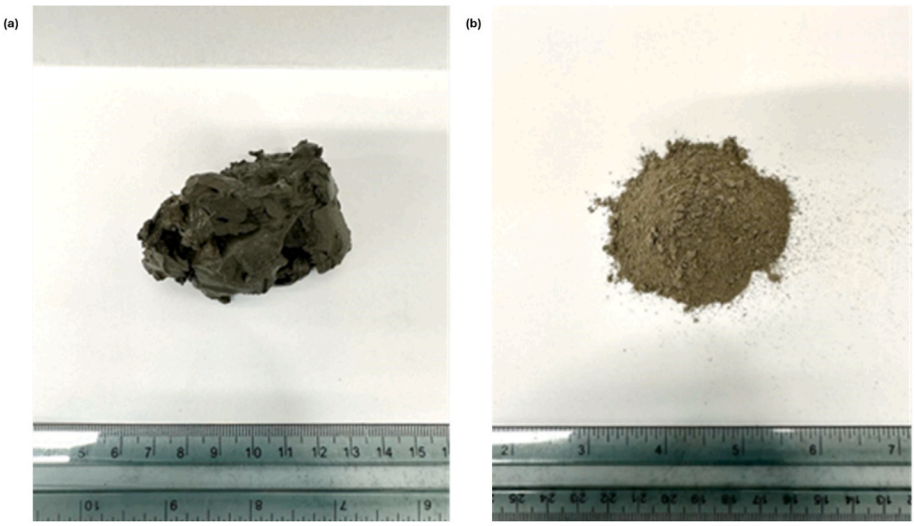

Fig. 2. Finnish clay (a) as received and (b) after milling.

1.1. Research significance

Fewer studies have reported the influence of BA on the performance of clay bricks, but no investigation has been conducted on the influence of BA addition on the performance of clay bricks using different types of clay (kaolinitic and illitic) as precursors. In this study, a comprehensive experimental program was designed to investigate for the first time the effects of substituting 0–30 wt% of either kaolinitic or illitic clay with BA on the mechanical, microstructural, and durability properties of clay bricks. This study suggests that using BA as an additive not only serves as a potential method for their valorization but can also lower the firing temperature and enhance the properties of clay bricks. The results of this experimental study highlight the potential for the reuse of BA in clay-bonded bricks for construction applications.

2. Experimental work

2.1. Materials

Two types of clay and BA were used as precursors to prepare the bricks. The first clay is called London clay (named "LC") because it originates in London. It is a kaolinitic clay and was supplied in a semi-dry state by Tiileri Oy (Finland). The clay was dried in an oven at 60 °C for 24 h before use (Fig. 1). The second clay used is called Finnish clay (named "FC") because it originates in Finland. It is an illitic clay supplied in a slurry form by Leca Oy (Finland). The clay was dried in an oven at a temperature of 60 °C for 48 h before use (Fig. 2). BA used as admixture was supplied in a moist granular form and was dried in the oven at a temperature of 60 °C for 24 h to remove the residual moisture. After drying, the as-received BA was sieved through a 2-mm mesh to remove any unwanted materials, such as glass or metal that might interfere with the firing process. Before the use of FC and LC as precursors for brick production, they were milled for 3 h in a tumbling ball mill (10 L, TPR-D-950-V-FU-EH, 85 rpm, Germatec, Germany) using 150 stainless steel balls of optimized sizes (45 balls of 40 mm Ø, 45 balls of 30 mm Ø, and 60 balls of 25 mm Ø). The 10-L jar was loaded with 2 kg FC or LC for each milling batch. Alternatively, the BA used in this study was used without the need for milling because it has a suitable particle size for sand replacement, which is a common opening agent in brick production. In addition, by using BA as received, the energy consumption associated with the communition process and the milling cost are avoided.

The chemical compositions of FC, LC, and BA were determined using X-ray fluorescence spectroscopy (XRF, Axios mAX; Malvern PANalytical, UK) from a melt-fused tablet. The density of the materials was measured using a helium pycnometer (Micrometrics, USA), and the average of five consecutive density measurements was taken as the density value. The chemical compositions and densities of the materials are listed in Table 2.

Table 1
Mix design of the prepared brick samples. The values are given in grams (g).

Ref	LC	FC	BA	Water
LC100	100			12
LC90BA10	90		10	12
LC80BA20	80		20	12
LC70BA30	70		30	12
FC100		100		12
FC90BA10		90	10	12
FC80BA20		80	20	12
FC70BA30		70	30	12

The particle size distributions of the milled FC and LC as well as the as-received BA was analyzed with a laser diffraction technique (Beckman Colter 13,320, USA) using the Fraunhofer model. During particle size measurements, isopropanol was used as a dispersion medium for the samples to prevent reactions with water. Three replicate measurements were performed for each sample to ensure the reliability of the results. The average particle size distributions are presented in Fig. 5. The plasticity index of the clay samples was determined using the Atterberg limits. Using the Casagrande cup method, the clay was prepared in a paste form and placed in the cup, and a groove was made at the center. After 25 blows with a liquid limit device, the limit is defined as the moisture content (in percentage) required to close 0.5 inches along the bottom of the groove. The plasticity index of FC and LC was determined by calculating the variance in the moisture content between its liquid limit, i.e., the point at which it transitions from a liquid to a plastic consistency at a higher moisture level, and its plastic limit, i.e., the point at which it shifts from a plastic to a solid consistency at a lower moisture level.

2.2. Sample preparation

We prepared eight different mixes, as shown in Table 1. Two reference samples were prepared with 100 wt% FC or LC, and the remaining six samples were blended matrices prepared by replacing 10, 20, and 30 wt% FC or LC with BA. The samples were mixed in a high-shear mixer (IKA Eurostar 20; IKA Staufen, Germany). The dry powders were first mixed for 2 min at 500 rpm; then, an appropriate amount of deionized

water was added and further mixed for 5 min at 1000 rpm until a homogenous mixture was achieved. Using the same mixing procedure, reference samples made of only FC and LC were also prepared. The bricks were cast into a 50 mm–diameter mold (50 × 100 mm) fitted to the briquette machine and pressed using a laboratory cold-press briquetting machine. It is worth mentioning that the moisture content and briquetting force play important roles in influencing the properties of bricks. Therefore, the water content was fixed at 0.12 (i.e., 12 g of water per 100 g of dry matter), and the briquetting pressure was fixed at 100 bar for all the samples based on the optimized result from the preliminary experiment. The dimensions of the bricks before firing are 50 × 50 mm, and 20 samples per mix were produced. The prepared samples were dried in an oven at 60 °C for 24 h, followed by drying at 100 °C for 24 h. The samples were heated at 1000 °C in an electric furnace (ENTECH, Sweden) at a constant rate of 5 °C/min. The firing temperature selection was based on the optimization process in the preliminary experiment and other studies related to the use of BA in bricks [26,30]. Once the target temperature had been reached, it was maintained for 2 h to allow for thermal homogenization in the sample cross-section. After firing, the samples were allowed to cool freely in the furnace to prevent thermal shock. The visual appearance (color change and macro cracks), residual compressive strength, mass loss, shrinkage, and microstructural changes were determined after exposure to thermal loads.

2.3. Materials characterization and methodology

2.3.1. XRD analysis

The mineralogical compositions of the precursors and bricks were determined using an XRD spectrometer (Rigaku Smartlab diffractometer). The analysis was performed at 135 mA and 40 kV using Cu K-beta radiation with a scanning rate of 0.02° 2θ/step between 5° and 80°. The crystalline phases were quantified by applying the Rietveld refinement method after incorporating 10 wt% rutile (TiO_2) as the internal standard.

2.3.2. TG/DSC analysis

The TG/DSC measurements of LC, FC, and BA were performed using a NETZSCH STA 449F3 TG/DSC instrument at a constant heating rate of 5 °C/min. The samples were heated from room temperature to 1000 °C in an air atmosphere.

2.4. Characterization of the fired brick

2.4.1. Mass loss

The change in the mass of the samples before and after firing was calculated using the following equation:

$$\Delta M = \frac{M_f - M_o}{M_o} \times 100,$$

where M_f is the mass of the specimen after firing (kg) and M_o is the initial mass (kg) of the specimen at the initial state (before firing).

2.4.2. Linear shrinkage

The linear shrinkage of all samples was performed to determine the change in length. The initial length measured before firing was taken as the initial length (L_o), whereas L_t was taken as the length after firing. The change in length due to shrinkage is calculated as follows:

$$\Delta L = \frac{L_0 - L_t}{L_i} \times 100,$$

where L_i is nominal effective length of the mold.

2.4.3. Compressive strength

To determine the influence of BA addition on the mechanical properties of the brick samples, compressive strength tests were performed using a Zwick testing machine (Zwick Roell Group, Ulm, Germany) with a maximum load of 100 kN and a loading force of 2.4 kN/s. For each composition, the average of the four values was taken as the representative value of its compressive strength. The error bars in the compressive strength measurements indicate the standard deviation among the measured values. The compressive strength was determined using the following equation:

$$\sigma = P/A,$$

where σ is the compressive strength in N/mm^2, P is the load or force in N, and A is the cross-sectional area in mm^2.

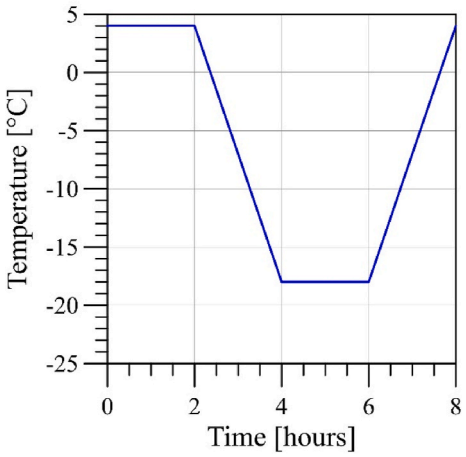

Fig. 3. One-cycle program in freeze–thaw.

2.4.4. Water absorption and apparent density

The water absorption of the brick samples after firing was carried out in accordance with the ASTM C642 recommendations. Triplicate samples for each mix composition were immersed in deionized water at room temperature and analyzed after 24 h to determine the continuous absorption of water into the samples. The average of the three sample measurements was calculated and reported for each data point. The water absorption was then calculated using the following equation:

$$\text{Water absorption } (\%) = \frac{M_s - M_D}{M_D} \times 100,$$

where M_S is water-saturated surface dry mass in air and M_D is oven dry mass in air.

The apparent density was determined using the Archimedes principle in accordance with the SFS-EN 1936 standard.

2.4.5. Leaching

The leaching and environmental analysis was carried out on the BA and brick samples in accordance with European standard EN 12457–2 [31]. After firing, the brick samples were crushed and sieved to particle sizes below 4 mm. The sieved samples were mixed with pure water at a liquid–solid weight ratio of 10 and were rotated for 24 h at 30 rpm in a rotary tumbler (Retsch, Germany). After rotation, the mixture was filtered through a 0.45 μm membrane filter under vacuum, and the filtrate was collected in a conical flask. Additionally, the pH and conductivity of the filtrate were measured. The filtrate was acidified with HNO_3, and the concentration of the leached elements was determined by inductively coupled plasma mass spectrometry.

2.4.6. Freeze–thaw resistance

The freeze–thaw resistance of the brick samples was tested in accordance with ASTM C666/C666M − 15 [32]. Three brick samples for each mix were immersed in tap water in a plastic container and placed in a climate chamber (WK3-180/40, Weiss Technik, Grand Rapids,

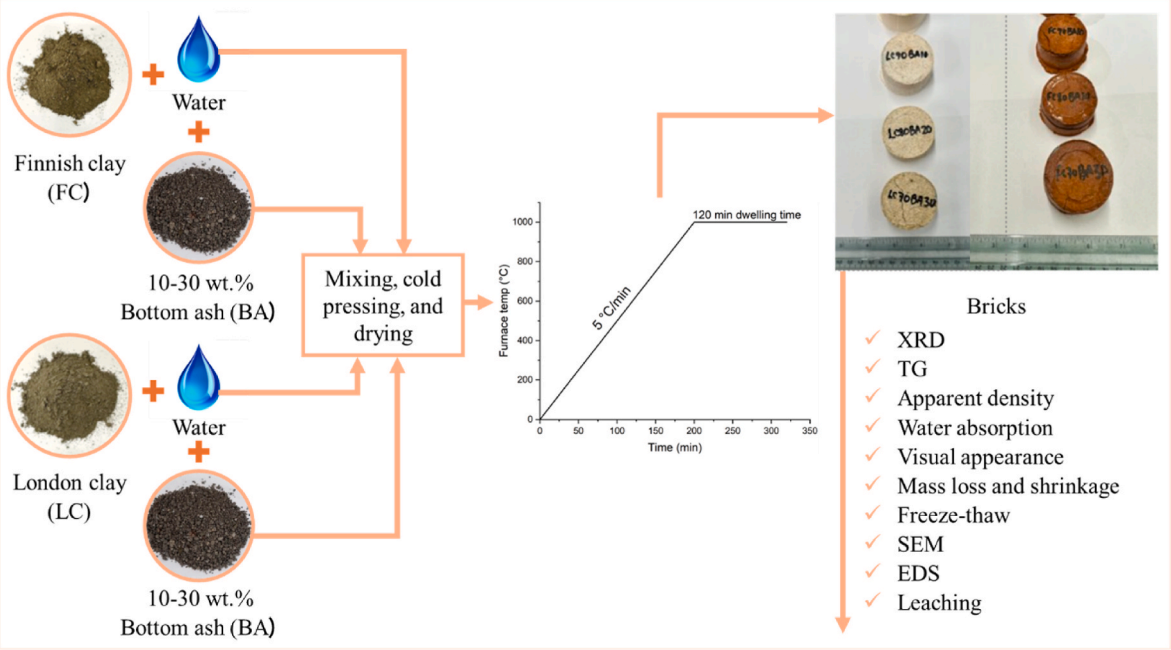

Fig. 4. Sketch of production methodology.

Germany). The water level was kept constant throughout the thawing period, and 50 freeze–thaw cycles were conducted. The temperature of one cycle was from −18 °C to +4 °C, and the duration of each cycle was 8 h. This means that one cycle (8 h/cycle) consisted of a dwell time of 2 h at +4 °C, 2 h for lowering the chamber temperature to −18 °C, a dwell time of 2 h at −18 °C, and 2 h for raising the chamber temperature to +4 °C. A schematic of the one-cycle program is shown in Fig. 3. The residual compressive strength was measured after 50 freeze–thaw cycles.

2.5. SEM-EDS

The morphologies of the prepared bricks were investigated by SEM-EDS analysis (Zeiss Ultra Plus, Germany). The fractured surfaces of the samples were analyzed using a backscattered electron detector with an acceleration voltage of 15 kV and a working distance of approximately 8.2 mm.

2.6. The experimental design

The experimental plan is summarized in Fig. 4.

3. Results and discussion

3.1. Characterization of the raw materials

The particle size distribution curves of the raw materials are presented in Fig. 5. All materials showed different particle size distributions. LC and FC had similar particle size distributionss, with median particle sizes (d_{50}) of 4 and 6 μm, respectively. The particle size distribution of LC and FC is sufficiently fine to be used as a precursor for brick production. In contrast, BA contains coarser particles with a d_{50} of 216 μm and is therefore used as an opening agent for bricks rather than sand. Because of the grain size of BA, its incorporation can improve the packing density and pore structure.

The chemical compositions and densities of the raw materials are listed in Table 2. LC, FC, and BA are rich in SiO_2 and Al_2O_3, constituting >70 % of the weight content of all samples. In addition, FC and BA have higher alkali oxides (Na_2O and K_2O) contents than LC. The presence of a high alkali content can act as a flux during brick production. In addition, BA is rich in CaO, whereas FC is rich in Fe_2O_3. The difference in the chemical composition of the precursors is expected to influence the properties of the bricks produced.

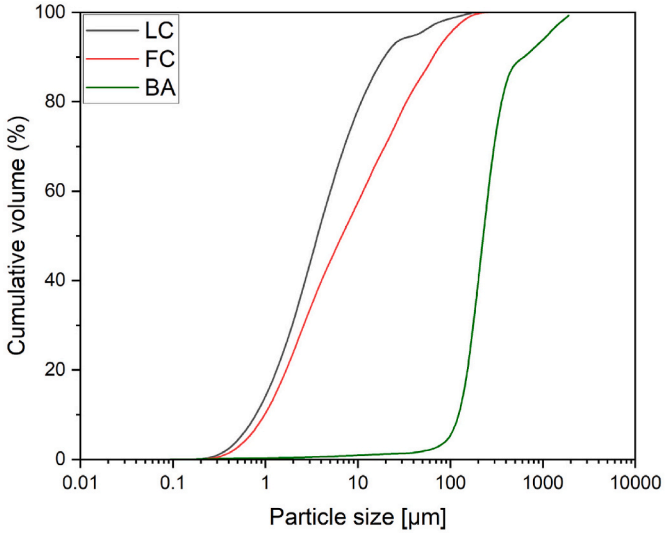

Fig. 5. Particle size distributions of London clay, Finnish clay, and bottom ash.

The mineralogical phases of FC, LC, and BA are presented in Fig. 6. The XRD analysis showed that the main crystalline components of the FC were quartz (pdf. 04-008-8228), muscovite (pdf. 04-017-9606), and illite (pdf. 04-016-2978). The LC consisted of kaolinite (pdf. 01-079-6476), quartz (pdf. 04-003-6495), and muscovite (pdf. 04-012-1905). Conversely, the BA consisted of anorthite [$CaAl_2Si_2O_8$) pdf. 04-021-5177], anorthoclase [$(Na_{0.75}K_{0.25})$ $(AlSi_3O_8)$ pdf. 01-075-1633], quartz [(SiO_2) pdf.04-014-7568], orthoclase [$(KAlSi_3O_8)$ pdf. 01-071-1543], and calcite [$(CaCO_3)$ pdf. 04-006-6528].

The TG curves of LC and FC showed gradual mass loss from 24 °C to 400 °C, followed by an intense mass loss from 400 °C to 1000 °C (Fig. 7). The endothermic peak observed at 500 °C can be ascribed to the

Table 2
Chemical compositions and densities of FC, LC, and BA.

	FC	LC	BA
SiO_2	51.2	54.6	64.3
Al_2O_3	18.9	27.2	10
Fe_2O_3	12.7	1.4	3.2
CaO	2.0	0.3	12.1
MgO	4.7	0.4	2.3
Na_2O	2.3	0.3	3.0
K_2O	3.7	1.8	3.5
TiO_2	1.0	1.2	0.8
P_2O_5	0.14	0.05	0.74
MnO	0.16	0.04	0.39
SO_3	0.07	0.5	0.4
Density (g/cm^3)	2.8	2.3	2.8

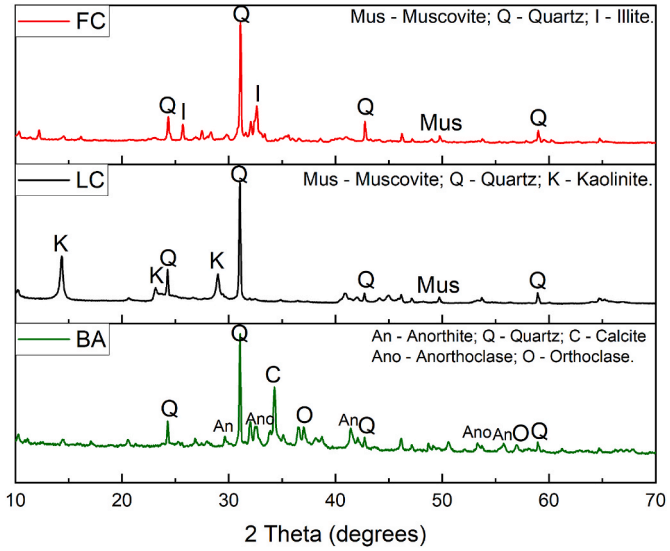

Fig. 6. X-ray diffraction patterns of Finnish clay, London clay, and bottom ash.

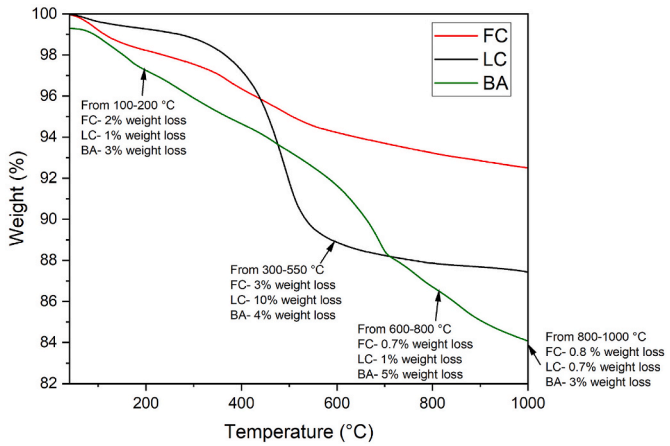

Fig. 7. Thermogravimetry curves of Finnish clay, London clay, and bottom ash.

Table 3
Plasticity indices of the clays used.

Clay type	Plastic limit (%)	Liquid limit (%)	Plasticity index (%)
LC	24.5	45.5	20.9
FC	30.8	47	16.2

dehydroxylation of kaolinite and illite, respectively [33]. The thermal behaviors of LC and FC are similar to those of other kaolinitic and illitic clays reported in previous studies [34]. Alternatively, a gradual mass loss was observed in the TG curve of BA from 24 °C to 650 °C, which was likely attributed to the loss of moisture and calcination of the unburnt organic matter. This is followed by another mass loss from 650 to 1000 ascribed to the decarbonation of carbonate phases such as calcite [35], which is consistent with the XRD results.

The plasticity indexes of the clays are presented in Table 3. The results show that FC and LC can be classified as moderately plastic with a plasticity index in the range of 16%–21 % and a liquid limit in the range 45%–47 %. This indicates that FC and LC have a moderate affinity for water and can change their volume and shape in response to variations in water content. FC and LC have a balanced combination of plastic and non-plastic properties.

3.2. Performance of the brick incorporating incinerated BA

3.2.1. Visual observation of the prepared bricks

The physical appearance of the bricks in Fig. 8 shows that the FC-based bricks are red in color, whereas those of the LC-based bricks vary from white to light brown. The red color observed in the FC-based bricks (Fig. 8a) can be attributed to the phase transformation and oxidation of the mineral constituents, possibly iron compounds [36]. This is consistent with those reported in the literature where the oxidation of iron compounds and red color was observed when clay and other slags containing more than 4 wt% iron in their bulk chemical composition were fired at high temperatures [36,37]. In this study, the FC used had 12.7 wt% iron in its bulk chemical composition, which can explain the redness of the FC-based bricks. Alternatively, the color of the LC-based bricks varied from white to light brown because of the phase transformation that occurred with the incorporation of BA (Fig. 8b). The details of the mineralogical transformations of the bricks after firing at elevated temperatures are explained in section 3.3.1. The color difference between FC- and LC-based bricks can be attributed to the low iron content in LC.

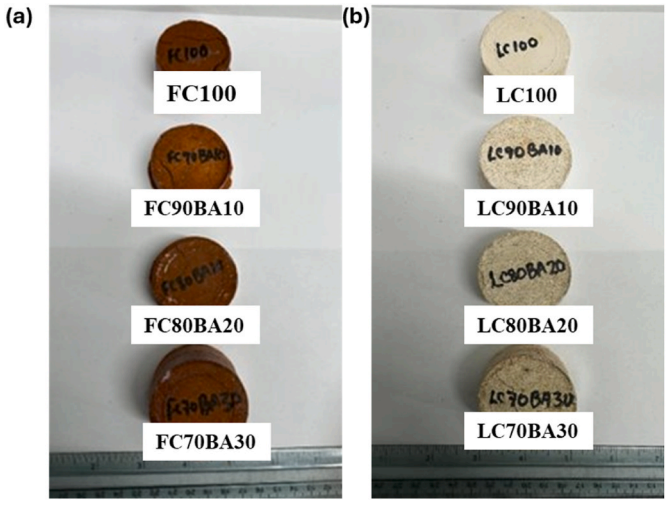

Fig. 8. Physical appearance of the prepared bricks; (a) FC- and (b) LC-based bricks.

3.2.2. Mechanical properties

The compressive strengths of the brick samples before and after firing are presented in Fig. 9. The results show that the green strength (before firing) of the reference LC (LC100) and the samples containing BA (LC90BA10, LC80BA20, and LC70BA30) is the same (2 MPa), indicating that the incorporation of BA does not have any effect on the green strength of the samples (Fig. 9a). Meanwhile, the obtained green strength is strong enough to be transferred to the furnace without breaking, making it suitable for industrial operations using continuous drying and low stress before firing. However, after firing, the compressive strength of all samples increased, but the percentage increase varied among the samples. The compressive strength of the LC-based bricks increased with increasing BA content up to 20 wt%, after which it remained stable, suggesting that 20 wt% replacement of LC with BA could be the optimum replacement level. The results obtained in this study are consistent with those reported in the literature when BA was combined with clay to produce ceramic tiles [38]. Brick made of London clay with 20 % BA (LC80BA20) exhibited the highest compressive strength (17 MPa), whereas LC100 made with 100 % London clay exhibited the lowest compressive strength (12 MPa). The high strength of LC80BA20 can be attributed to the effect of BA during firing. The dual effect of elevated temperature exposure and BA incorporation is presumed to have enhanced the formation of more stable crystalline phases such as anorthite and nepheline (section 3.3.1) and densified the structure of the bricks at 1000 °C.

For the FC-based bricks, the compressive strength of the green formulations (before firing) varied among the samples, with FC100 having the highest green strength (8 MPa), whereas the lowest green strength occurred in FC80BA20 (2 MPa) (Fig. 9b). After firing, the compressive strength of the FC-based bricks increased with an increase in the BA content up to 10 wt%, after which it started to decrease, suggesting that the 10 wt% replacement of the FC with BA may be the optimum replacement level. FC90BA10 had the highest compressive strength (19 MPa), whereas FC100 had the lowest compressive strength (12 MPa). Comparatively, the difference in the compressive strength trends between the FC- and LC-based bricks can be ascribed to the difference in the sintering behavior and chemical and mineralogical composition of the FC and LC, more notably, the higher content of alkali oxides (K_2O and Na_2O) in the FC compared to the LC. In accordance with the ASTM C62 specifications for compressive strength [39], the strength of the building bricks should be 10.3, 17.2, and 20.7 MPa for negligible weathering, moderate weathering, and severe weathering, respectively. With reference to this standard, all the samples meet the compressive strength requirements of bricks subjected to negligible weathering, whereas only the compressive strength of FC90BA10 meets the requirements specified for bricks subjected to moderate weathering [39].

3.2.3. Mass loss and linear shrinkage

The mass loss caused by exposure to elevated temperature is presented in Fig. 10. For FC- and LC-based bricks, the mass loss was reduced by BA incorporation. The incorporation of BA into the clay mixtures is presumed to have influenced a combination of physicochemical processes occurring in the brick body during sintering, such as dehydration of minerals, diffusion processes, recrystallization, and the formation of new minerals, deformation of carbonate phases into CO_2, and volatilization of organic matter. Moreover, the lower mass loss observed in samples containing BA may also be because of the formation of the liquid phase caused by the high alkali oxides content in BA, which resulted in the convergence of particles, lowered the porosity, and enhanced the densification of the bricks. In addition to LC100 and FC100, the mass loss of samples containing BA remained in the range often observed for normal clay bricks (15 %) [25].

Linear shrinkage usually occurs in brick samples at high temperatures because of dehydration, dehydroxylation, phase decomposition,

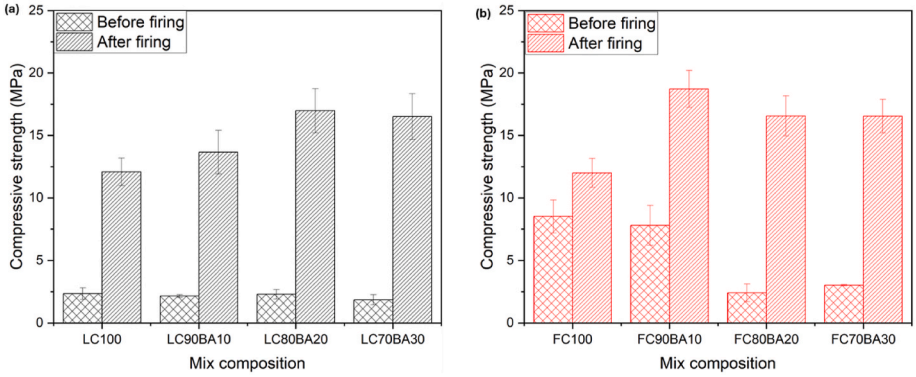

Fig. 9. Compressive strength of the brick samples.

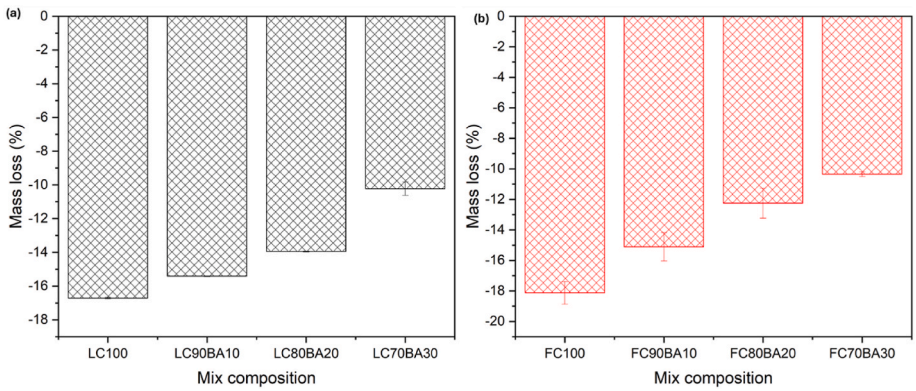

Fig. 10. Mass loss of the brick samples.

Table 4
Linear shrinkage of the brick samples.

	LC100	LC90BA10	LC80BA20	LC70BA30	FC100	FC90BA10	FC80BA20	FC70BA30
Shrinkage (%)	4.4	4.4	3.7	3.5	12	8.7	4.6	4.5

and liquid phase formation [34]. As reported in the literature, the shrinkage of a good-quality brick should be below 8 % [34]. As shown in Table 4, the incorporation of BA resulted in lower shrinkage values regardless of the clay used. The lower shrinkage values exhibited by the samples containing BA may be attributed to the presence of coarse quartz, which acts as an opening agent. A similar reduction in shrinkage was observed when coarse quartz feldspar sand was incorporated into clay mixtures for the production of building ceramics [37]. For the LC-based bricks, LC100 exhibited the highest shrinkage (4.4 %), whereas LC70BA30 exhibited the lowest shrinkage (3.5 %). Alternatively, for the FC-based bricks, FC100 exhibited the highest shrinkage (12 %), whereas FC70BA30 exhibited the lowest shrinkage (4.5 %). Because the FC- and LC-based bricks were fired at the same temperature, the higher shrinkage in FC100 compared with LC100 may be due to differences in the sintering behavior and chemical and mineralogical composition. Kaolinitic clays have one water layer, whereas illitic clays have two water layers [40]. Thus, the higher shrinkage of FC100 may be due to the higher dehydroxylation effect on the stability of FC100 compared to LC100, which causes water molecules to evaporate, resulting in the collapse of the clay mineral structure. As reported in the literature, the use of illitic clay in brick production can cause unwanted shrinkage and cracking during the drying and firing processes [41], and this may have been the case for the FC used in this study. The reduction resulting from BA incorporation was more visible in the FC-based bricks. The drastic reduction from 12 % for FC100 to 4.5 % for FC70BA30 is due to the synergistic effect of FC and BA, resulting in the formation of more closed pores and densification. FC and BA contain a high amount of alkali oxides, which can act as fluxing agents and contribute to the formation of closed pores and densification at high temperatures. Except for FC100 and FC90BA10, all remaining samples had shrinkage values below 8 %, which is consistent with the generally accepted requirement for fired bricks [42].

3.2.4. *Water absorption and apparent density*

The water absorption spectra and apparent densities of all samples are presented in Figs. 11 and 12. The water absorption of bricks is one of the most important properties because the less water that infiltrates the brick, the higher the durability and resistance to the natural environment. As observed in this study, regardless of the clay content, the water absorption of the bricks decreased with increasing BA content. The water absorption values varied from 3 % to 16 % for the FC-based bricks and from 16 % to 25 % for the LC-based bricks. One possible explanation could be that the addition of BA enhanced liquid phase formation, which contributed to the decrease in the porosity and water absorption rate. Comparatively, the lower water absorption values achieved in the FC-based bricks compared with the LC-based ones could be ascribed to the differences in the sintering behavior of both types of clays. The sintering (densification) of illitic clays occurs at much lower temperatures than that of kaolinitic clays. This is because alkali oxides, such as Na and K, present in illite through isomorphism or interlayer bonding can act as fluxing agents to reduce the sintering temperature and enhance liquid-state sintering [40]. For example, a study by Tominc et al. [43] confirmed that the densification of kaolinitic clay starts at approximately 200 °C higher that for illitic type of clay.

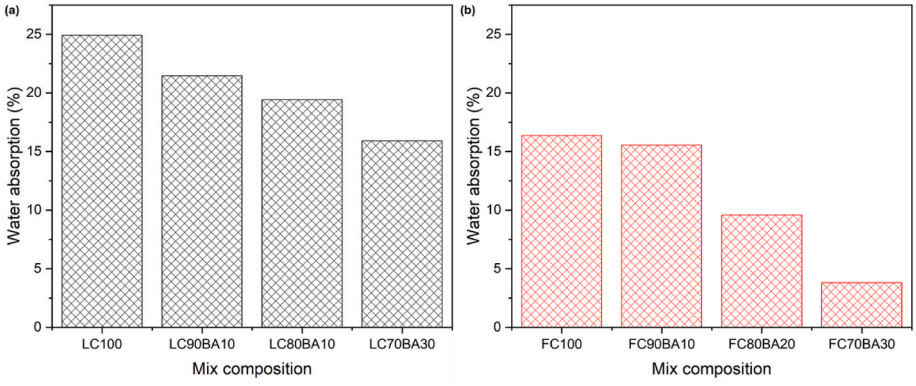

Fig. 11. Water absorption of the brick samples.

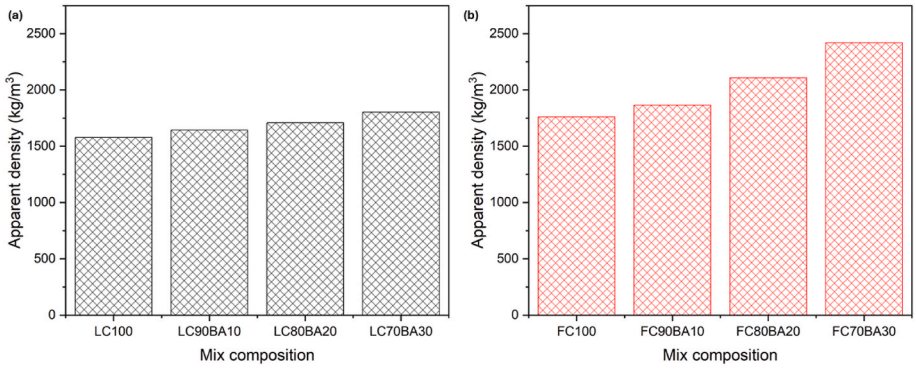

Fig. 12. Apparent densities of the brick samples.

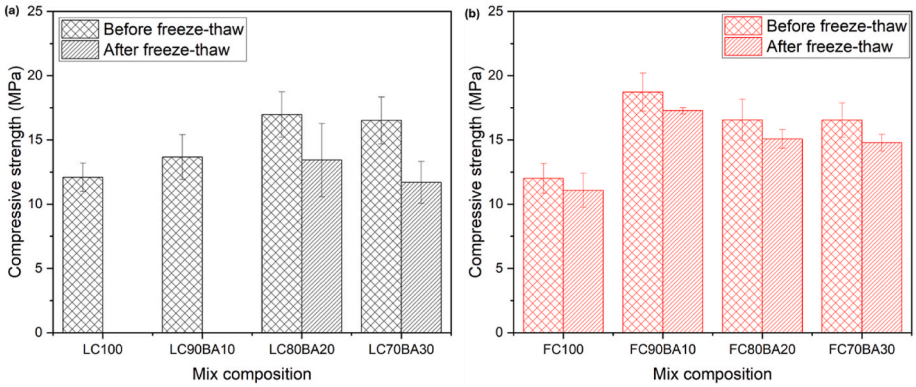

Fig. 13. Compressive strengths of the brick samples before and after freeze–thaw.

The compact and dense microstructures of the FC-based samples were in line with their higher compressive strength (Fig. 9). ASTM C62-23 specifies that the water absorption percentage of building bricks should not exceed 17 % for them to be used in extreme conditions [39]. Hence, all the FC-based bricks (FC100, FA90BA10, FC80BA20, and FC70BA30) and only one LC-based brick (LC70BA30) met the requirements. This indicates that compared with LC, the synergetic mixture of the FC and BA is beneficial for the water absorption properties of the bricks.

The apparent density results of the bricks are presented in Fig. 12. Regardless of the clay content, the apparent density of the bricks increased with increasing BA content. One possible explanation could be that an increase in the BA content in the ceramic body is presumed to have increased the apparent density of the samples. These results are consistent with the microstructure, water absorption, and mechanical properties of clay mixtures containing BA, indicating that BA incorporation is beneficial for matrix densification. The trend observed for apparent density and compressive strength indicates that the compressive strength of the samples was greatly influenced by the densification, which is in agreement with previous studies [42]. The increase in apparent density and decrease in water absorption observed with BA incorporation are comparable to the effects of BA addition in the production of fired clay bricks previously reported [42].

3.2.5. *Freeze–thaw*

The freeze–thaw test was performed on the brick samples to assess their residual mechanical properties (Fig. 13). All samples exhibited good stability after 50 freeze–thaw cycles, except for LC100 and LC90BA10, which were destroyed after exposure to freeze–thaw. For the FC-based bricks, the compressive strengths before exposure were 12, 19, 17, and 17 MPa for FC100, FA90BA10, FC80BA20, and FC70BA30, respectively. Meanwhile, after exposure to freeze–thaw, the residual compressive strength of the samples decreased to 11, 17, 15, and 15 MPa for FC100, FA90BA10, FC80BA20, and FC70BA30, respectively (Fig. 13b). For the LC-based bricks, the compressive strengths of LC100, LC90BA10, LC80BA20 and LC70BA30 were 12, 14, 17 and 17 MPa, respectively. After exposure to freeze–thaw, the compressive strengths of LC100 and LC90BA10 could not be measured because of complete disintegration, whereas those of LC80BA20 and LC70BA30 decreased to 13 and 12 MPa, respectively (Fig. 13a).

In general, the freeze–thaw resistance depends on three main factors; one is the strength of the material, which needs to be high enough to resist the ice-expansion force, the second is the porosity, as with lower porosity, less water enters the structure, and the third, very important one, is the pore size distribution. It has been recognized that a certain percentage of pores is greater than 3 m, which can contribute to better freeze–thaw performance [44].

The lower residual compressive strength exhibited by these samples after exposure to freeze–thaw conditions in water was likely due to the volume expansion of the absorbed water in the pores. It is well-known that the infiltration of water molecules inside the pore cavities of bricks weakens their structure, resulting in poor mechanical properties [45]. The absorption of this water is likely to increase, especially in samples that are more porous. The effect of the freeze–thaw cycles was more significant in LC100 and LC90BA10, causing physical damage, cracks, and eventual collapse of the bricks. One possible explanation could be that the microstructure of the LC100 and LC90BA10 bricks is weak, likely because they are not yet optimally sintered, allowing water to penetrate and become frozen and saturated, thus making them less durable. These results are in line with the SEM results shown in Fig. 15. The high stability of the FC-based bricks (FC100, FA90BA10, FC80BA20, and FC70BA30) and some LC-based bricks (LC80BA20 and LC70BA30) after exposure to 50 freeze–thaw cycles suggests that the prepared bricks have the potential to withstand severe weathering conditions.

Table 5
EN 12457–2 batch leaching test results of selected brick samples compared with the EU landfill directive indicative values for inert and nonhazardous waste. The results are the averages of two replicates, and the concentrations are presented as mg/kg.

Hazardous elements	Inert waste threshold	Nonhazardous waste threshold	LC70BA30	FC70BA30	BA
pH	N/A	N/A	10.16	9.67	11.48
Conductivity [mS/cm]	N/A	N/A	0.108	0.155	0.73
As	0.5	2	1.8	0.3	0.14
Ba	20	100	0.19	<0.06	3.1
Cd	0.04	1	<0.002	<0.002	<0.002
Cr	0.5	10	0.46	0.41	0.45
Cu	2	50	<0.01	<0.01	<0.01
Ni	0.4	10	<0.01	<0.01	<0.01
Pb	0.5	10	<0.004	<0.004	0.015
Sb	0.06	0.7	0.096	0.018	0.76
V			5.9	20	0.26
SO_4^{2-}	1000	20,000	150	400	490

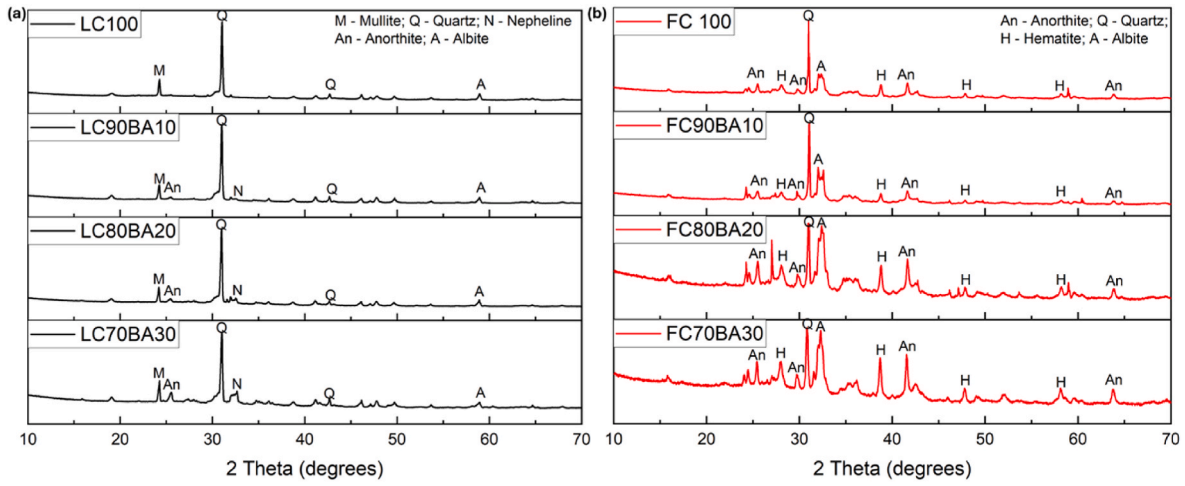

Fig. 14. X-ray diffraction patterns of the prepared bricks.

3.2.6. Leaching behavior

The leaching test results are presented in Table 5. The concentration of Sb in the BA eluate exceeded the regulatory limit for both inert and nonhazardous waste specified by the EU landfill directive. This may have been due to the presence of fine BA particles that increased the specific contact with the leaching solution. However, the concentration of other hazardous elements in BA is below the regulatory limit for inert and nonhazardous waste. Interestingly, the leaching values of Sb and other hazardous elements in the selected bricks with the highest BA content were below the limit values for inert and nonhazardous waste specified by EU regulation, indicating that Sb was properly encapsulated in the brick matrix.

3.3. Mineralogical and microstructural characterization of the bricks

3.3.1. Mineralogical characteristics

The XRD analysis results of the bricks after firing are presented in Fig. 14. For the LC-based bricks, quartz, mullite, and albite phases were identified in the XRD patterns of all the samples, consistent with the mineralogy of the starting LC and BA (Fig. 6). However, no muscovite peak was observed in the brick samples, indicating the transformation of the muscovite into amorphous structures upon heating. In addition, a new crystalline peak of mullite appeared after firing, which was attributed to the decomposition of kaolinite. In fact, kaolinite first decomposes into amorphous metakaolin at approximately 750 °C, and it later transforms into crystalline mullite starting at 900 °C [33]. In contrast to LC 100, which had quartz, mullite, and albite as the main crystalline phase, the crystalline phases present in the LC samples containing BA (LC90BA10, LC80BA20, and LC70BA30) are slightly different and contain quartz, mullite, albite, nepheline, and anorthite. The appearance of anorthite in LC-based bricks containing BA is caused by the incorporation of BA, and the peak intensity increased with increasing BA content (Fig. 14a). Generally, alkali oxides, such as Na_2O and K_2O, present in BA are one of their most reactive constituents at high temperature, resulting in the formation of a liquid phase and a new crystalline phase, such as anorthite, consistent with those reported in the literature [42]. In addition, the formation of nepheline was also observed in LC-based samples containing BA, with the reflection patterns of nepheline being higher in LC70BA30 owing to the high BA content. Nepheline is a Na-silicate mineral that may have crystallized from the Na-rich clusters present in BA at high temperatures.

For FC, there exists no difference in the mineralogical composition between reference FC (FC100) and those containing BA (FC90BA10, FC80BA20, and FC70BA30) (Fig. 14b). Quartz, anorthite, albite, and hematite phases were identified in the XRD patterns of the reference FC (FC100) and samples containing BA (FC90BA10, FC80BA20, and FC70BA30). Compared with the mineralogical composition of the starting FC, no muscovite peak was observed in the brick samples, indicating their transformation into an amorphous structure upon heating. The appearance of hematite in the FC-based bricks is likely due to the high Fe content in the bulk chemical composition of the FC, which can undergo oxidation during brick firing as a result of the breakdown of clay minerals at 1000 °C. A similar oxidation of iron to hematite has also been observed when iron-rich materials, such as copper and fayalite slag, are sintered at high temperatures to produce ceramics [46]. However, the reflection patterns of hematite increased with increasing BA content. In addition, the incorporation of BA reduced the reflection of quartz and increased the reflection of albite, likely due to the instability of quartz in alkaline melt, converting them into albite [47]. The intensities of the albite peak increased with increasing BA content. The addition of BA is presumed to have increased the sodium content of the clay mixture, which is crucial for the formation of albite, resulting in the increased strength of the brick. The reflection pattern of the anorthite increased with increasing BA content, and its formation was similar to that observed in the LC-based bricks. However, the crystalline reflections of anorthite in the FC-based bricks is higher than those in the LC-based bricks because of the slightly higher amount of CaO in the FC, which can act as an auxiliary flux material during firing.

Based on the XRD analysis, it can be deduced that the difference in the phase transformation occurring in the FC- and LC-based bricks influenced their mechanical and microstructural properties (sections 3.2.2 and 3.3.2).

3.3.2. SEM-EDS

The microstructure of the prepared bricks is presented in Fig. 15. For all samples, matrix densification increased with increasing BA content. This densification can be ascribed to the partial melting of BA due to the high alkali oxide content in BA. The melted phase is presumed to have reacted with some phases in the clay, resulting in the densification of the matrix and the formation of stable crystalline phases (section 3.3.1). It is worth mentioning that the amount of the liquid phase formed in the material is influenced by the physical, chemical, and mineralogical composition of the starting material, as well as the firing temperature [33]. The lower porosity and microstructural densification brought about by the addition of BA are more obvious for the FC-based bricks than for the LC-based bricks, which is attributed to the higher content of alkali oxides in the FC and the sintering pattern of the clays. The difference in the microstructure influenced the properties of the bricks.

The EDS maps obtained from the selected points in the reference samples and samples with the highest BA contents are presented in

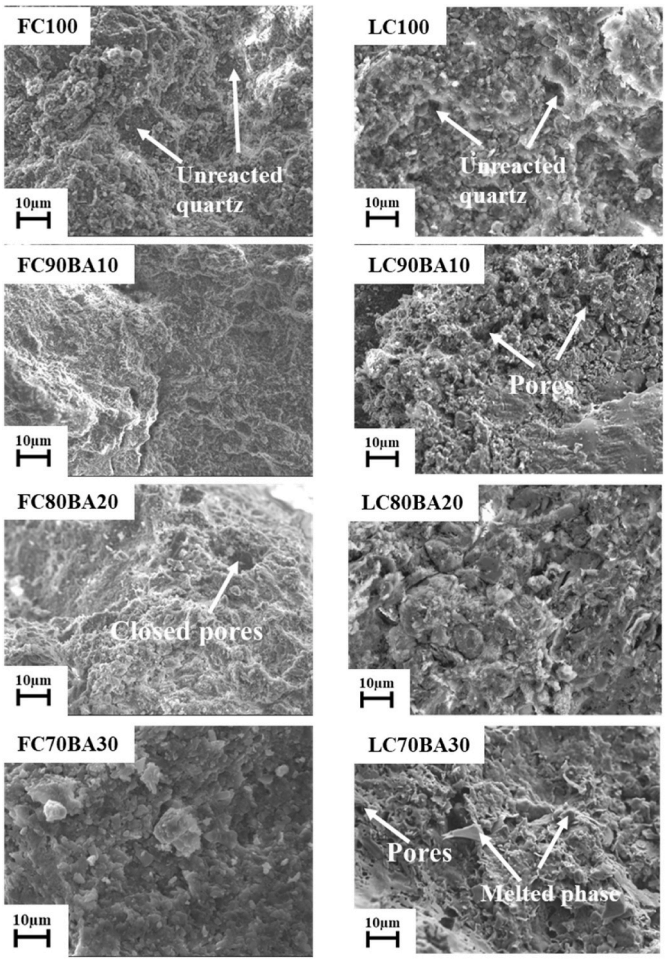

Fig. 15. SEM micrographs of the fractured surfaces of the reference samples and samples containing BA.

Fig. 16. The Ca, Al, Si, Na, and K contents of the specimens were also determined. Samples containing BA (FC70BA30 and LC70BA30) exhibited an even distribution of Na and K in the matrix compared with the reference samples (FC100 and LC100), indicating good dissolution and reactivity of Na and K from BA during firing. The Si map shows a more homogenous distribution in the FC-based bricks than in the LC-based ones. In addition, there exist some relics of Ca in samples containing BA, mainly originating from the added BA, with the effect being more visible in FC-based bricks. The better dissolution behaviors observed in the FC-based bricks can be ascribed to the better vitrification of the alkali-abundant FC, which contributes to the fluxing effect, favoring matrix softening and better element diffusion at high temperatures.

3.4. Discussion and comparative analysis

The results of this study demonstrate that incorporating BA into the LC and FC significantly influences the properties of the fired bricks. Specifically, the compressive strength of the LC-based bricks improved with increasing the BA content up to 20 %, whereas the FC-based bricks

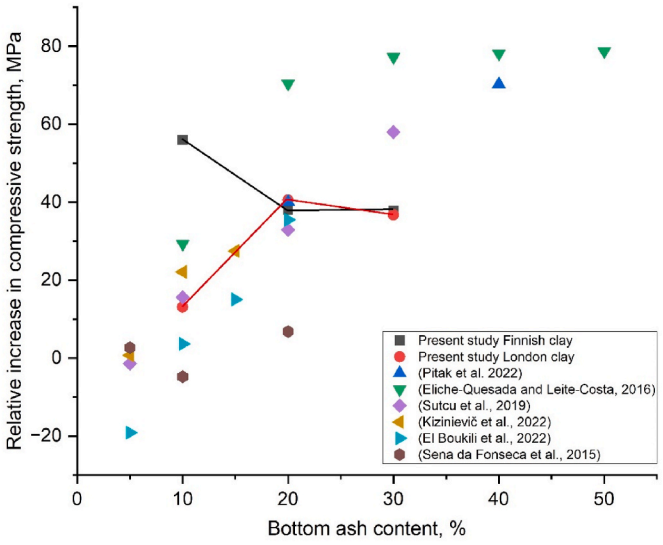

Fig. 17. Comparative analysis of the relative change in the compressive strength of brick samples with increasing BA content [26,30,48–51].

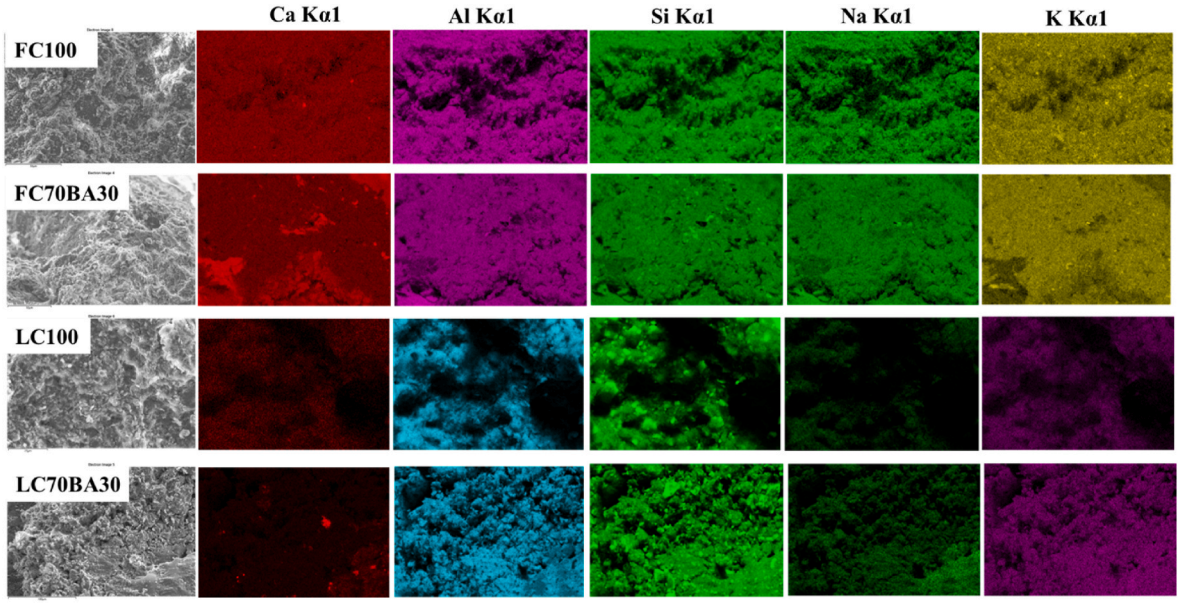

Fig. 16. EDS maps of the Ca, Si, Al, Na, and K brick samples.

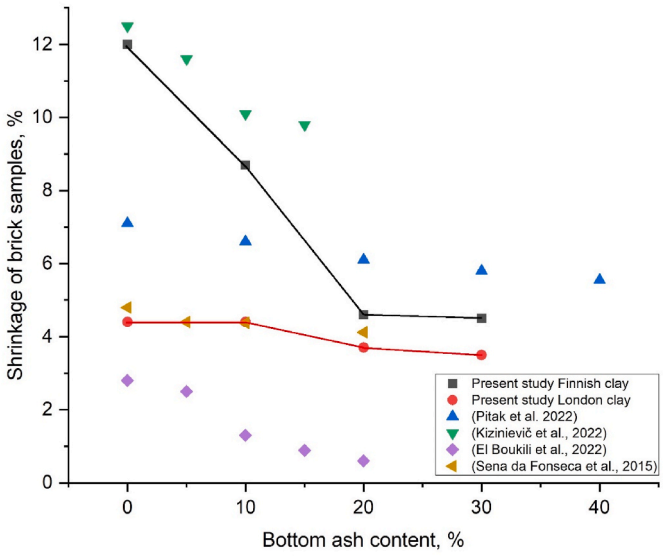

Fig. 18. Comparative analysis of the shrinkage of brick samples with different BA contents [30,48,50,51].

showed the optimal strength at 10 % BA. The comparative analysis and literature studies (Fig. 17) confirm that the incorporation of BA into the clay mixture generally enhances the compressive strength of the clay bricks. However, the extent of improvement in the compressive strength varies depending on the specific compositional mixes, materials, and types of BA used (such as MSWI bottom ash, co-combustion bottom ash, biomass bottom ash or coal combustion bottom ash) [26,30,48–51]. The study also observed that incorporating BA reduced the shrinkage in LC- and FC-based bricks, with a more pronounced effect in FC-based bricks, likely due to differences in their chemical and mineralogical compositions. This finding aligns with previous literature, as presented in Figs. 18 and 19, which also report a reduction in shrinkage when BA from various incineration sources (MSW, co-combustion of diverse materials, and industrial biomass incineration ashes) is added to the clay bricks. The reduction in the shrinkage of the clay bricks upon BA addition can be attributed to several factors. One key reason for this is that the organic matter present in BA is comparatively lower than that in clay, leading to a decrease in shrinkage when BA is added [26]. Additionally, the high alkali oxide content in BA can act as a fluxing agent, contributing to the formation of closed pores and densification at low firing temperatures. Because of the decreased shrinkage and densified structure, water absorption is reduced, and the apparent density of the clay bricks is increased with the addition of BA [30]. In line with this observation, a decrease in water absorption was noted for the bricks containing BA, which contrasts with a few studies that reported an increase in water absorption upon the addition of BA. In the above-mentioned study, the increase in water absorption was mainly attributed to the variation in the mineralogical composition and physical properties of BA and clay, as well as the compositional design of the clay bricks [26,30,48–51]. The reduction in water absorption with BA incorporation observed in this study is mainly attributed to the formation of a liquid phase during firing, leading to decreased porosity and, consequently, lower water absorption. The increased density and compact microstructure of BA-containing clay bricks, as shown in Figs. 12 and 15, further supports this explanation.

4. Conclusions

This study demonstrated the feasibility of using MSWI BA for clay-bonded bricks. The use of BA in brick production will eliminate the cost of landfilling. For instance, the landfilling cost of solid industrial waste in Finland is estimated to be 100€/ton. Crucially, reusing these industrial wastes can also reduce environmental degradation and pollution. FC is an illitic clay commonly found in Finland, whereas LC is a kaolinitic clay from London. These two types of clay are among the most commonly used in the brick industry. The BA used as the admixture has a high concentration of alkali oxides and is presumed to act as a fluxing agent when incorporated into the FC or LC. The fluxing effect of BA can lower the sintering temperature and consequently the energy demand and production cost of the produced bricks. The results show that BA addition benefits the mechanical and durability properties, with an increase in the compressive strength at 1000 °C. The addition of BA was observed to reduce the mass loss and firing shrinkage due to the presence of coarse quartz in BA, which acted as an opening agent. LC was less sensitive to the effect of BA because it had a lower alkali oxides content than FC. The green strength of the prepared bricks varied between 2 and 9 MPa, and the compressive strength of the fired bricks varied between 12 and 19 MPa. Meanwhile, the compressive strength values of some fired brick samples exceeded 17 MPa, thus satisfying the compressive strength requirement for bricks subjected to moderate weathering in accordance with the ASTM C62 standard. The water absorption percentages of the samples decreased with increasing BA content, with the FC-based bricks exhibiting the lowest water absorption. Except for LC100 and LC90BA10, which were destroyed after freeze–thaw, residual compressive tests of the remaining samples proved the stability of the materials after 50 freeze–thaw cycles, demonstrating

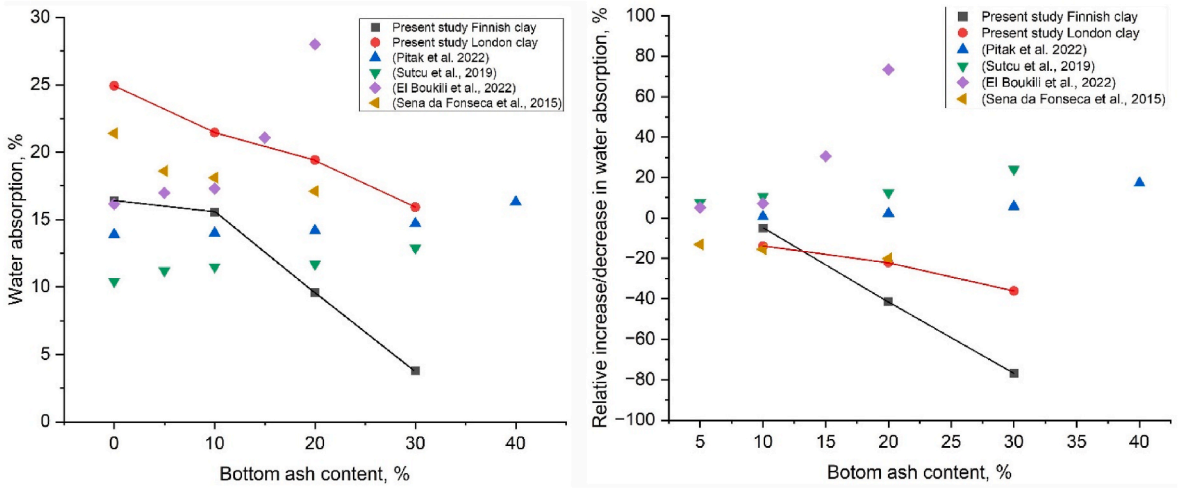

Fig. 19. Comparative analysis of the shrinkage of brick samples with different BA contents [30,48,50,51].

their potential suitability as construction materials for severe weathering environments. The Sb leaching values in raw BA exceeded the limit for inert and nonhazardous waste specified by the EU landfill directive. Meanwhile, the leaching value of Sb in the selected bricks with the highest BA content was below the limit values for inert and nonhazardous waste specified by the EU regulation, indicating that Sb was properly encapsulated in the brick matrix. These results provide insights into the feasibility of upcycling BA in clay-bonded bricks for potential construction applications. Future research directions include the characterization of other physical and technological properties such as porosity and thermal conductivity, and pilot-scale production with their cost–benefit analysis. The proper management and reuse of BA could also help improve social sustainability objectives.

CRediT authorship contribution statement

Adeolu Adediran: Writing – review & editing, Writing – original draft, Visualization, Validation, Supervision, Methodology, Investigation, Formal analysis, Data curation, Conceptualization. **Shaurin Maher Kikky:** Writing – review & editing, Writing – original draft, Validation, Investigation, Formal analysis, Data curation, Conceptualization. **Suman Kumar Adhikary:** Writing – review & editing, Writing – original draft, Methodology, Investigation, Formal analysis, Conceptualization. **Vilma Ducman:** Writing – review & editing, Validation, Investigation, Formal analysis, Conceptualization. **Priyadharshini Perumal:** Writing – review & editing, Writing – original draft, Validation, Project administration, Methodology, Investigation, Funding acquisition, Formal analysis, Conceptualization.

Declaration of competing interest

The authors declare no conflict of interest whatsoever.

Acknowledgements

This work is supported by the EU Horizon Europe project AshCycle (101058162) and Research council of Finland project SusRes (347678). Adeolu Adediran has received funding from Auramo Foundation for his postdoctoral research. The authors gratefully acknowledge the Center for Material Analysis, University of Oulu, Finland for assistance with data analysis.

References

[1] B. Chen, P. Perumal, F. Aghabeyk, A. Adediran, M. Illikainen, G. Ye, Advances in using municipal solid waste incineration (MSWI) bottom ash as precursor for alkali-activation materials: a critical review, Resour. Conserv. Recycl. 204 (2024) 107516, https://doi.org/10.1016/j.resconrec.2024.107516.

[2] C.C. Wiles, Municipal solid waste combustion ash: state-of-the-knowledge, J. Hazard Mater. 47 (1996) 325–344, https://doi.org/10.1016/0304-3894(95)00120-4.

[3] P. Tang, M.V.A. Florea, P. Spiesz, H.J.H. Brouwers, Application of thermally activated municipal solid waste incineration (MSWI) bottom ash fines as binder substitute, Cement Concr. Compos. 70 (2016) 194–205, https://doi.org/10.1016/j.cemconcomp.2016.03.015.

[4] P. Perumal, M. Illikainen, Feasibility study of one-Part Alkali activated material with MSWI fly ash, in: J.I. Escalante-Garcia, P. Castro Borges, A. Duran-Herrera (Eds.), Proceedings of the 75th RILEM Annual Week 2021, Springer International Publishing, Cham, 2023, pp. 579–585, https://doi.org/10.1007/978-3-031-21735-7_63.

[5] B. Chen, G. Ye, The role of water-treated municipal solid waste incineration (MSWI) bottom ash in microstructure formation and strength development of blended cement pastes, Cement Concr. Res. 178 (2024) 107440, https://doi.org/10.1016/j.cemconres.2024.107440.

[6] Y. Sun, B. Chen, S. Zhang, K. Blom, M. Luković, G. Ye, Characterization, pretreatment, and potential applications of fine MSWI bottom ash as a supplementary cementitious material, Construct. Build. Mater. 421 (2024) 135769, https://doi.org/10.1016/j.conbuildmat.2024.135769.

[7] B. Chen, Y. Zuo, S. Zhang, L.M. de Lima Junior, X. Liang, Y. Chen, M.B. van Zijl, G. Ye, Reactivity and leaching potential of municipal solid waste incineration (MSWI) bottom ash as supplementary cementitious material and precursor for alkali-activated materials, Construct. Build. Mater. 409 (2023) 133890, https://doi.org/10.1016/j.conbuildmat.2023.133890.

[8] B. Chen, P. Perumal, M. Illikainen, G. Ye, A review on the utilization of municipal solid waste incineration (MSWI) bottom ash as a mineral resource for construction materials, J. Build. Eng. 71 (2023) 106386, https://doi.org/10.1016/j.jobe.2023.106386.

[9] S.K. Adhikary, A. D'Angelo, V. Viola, M. Catauro, P. Perumal, Alternative construction materials from industrial side streams: are they safe? Energ. Ecol. Environ. 9 (2024) 206–214, https://doi.org/10.1007/s40974-023-00298-1.

[10] C. Ferreira, A. Ribeiro, L. Ottosen, Possible applications for municipal solid waste fly ash, J. Hazard Mater. 96 (2003) 201–216, https://doi.org/10.1016/S0304-3894(02)00201-7.

[11] K.E. Haugsten, B. Gustavson, Environmental properties of vitrified fly ash from hazardous and municipal waste incineration, Waste Manag. 20 (2000) 167–176, https://doi.org/10.1016/S0956-053X(99)00325-6.

[12] Q. Qiu, X. Jiang, S. Lu, M. Ni, Effects of microwave-assisted hydrothermal treatment on the major heavy metals of municipal solid waste incineration fly ash in a circulating fluidized bed, Energy Fuels 30 (2016) 5945–5952, https://doi.org/10.1021/acs.energyfuels.6b00547.

[13] Y. Luo, S. Zheng, S. Ma, C. Liu, X. Wang, Preparation of sintered foamed ceramics derived entirely from coal fly ash, Construct. Build. Mater. 163 (2018) 529–538, https://doi.org/10.1016/j.conbuildmat.2017.12.102.

[14] K.-S. Wang, C.-J. Sun, C.-C. Yeh, The thermotreatment of MSW incinerator fly ash for use as an aggregate: a study of the characteristics of size-fractioning, Resour. Conserv. Recycl. 35 (2002) 177–190, https://doi.org/10.1016/S0921-3449(01)00121-5.

[15] Z. Zhang, A. Li, X. Wang, L. Zhang, Stabilization/solidification of municipal solid waste incineration fly ash via co-sintering with waste-derived vitrified amorphous slag, Waste Manag. 56 (2016) 238–245, https://doi.org/10.1016/j.wasman.2016.07.002.

[16] C.R. Cheeseman, A. Makinde, S. Bethanis, Properties of lightweight aggregate produced by rapid sintering of incinerator bottom ash, Resour. Conserv. Recycl. 43 (2005) 147–162, https://doi.org/10.1016/j.resconrec.2004.05.004.

[17] S. Bethanis, C.R. Cheeseman, C.J. Sollars, Effect of sintering temperature on the properties and leaching of incinerator bottom ash, Waste Manag. Res. 22 (2004) 255–264, https://doi.org/10.1177/0734242X04045426.

[18] K.C.P. Faria, R.F. Gurgel, J.N.F. Holanda, Recycling of sugarcane bagasse ash waste in the production of clay bricks, J. Environ. Manag. 101 (2012) 7–12, https://doi.org/10.1016/j.jenvman.2012.01.032.

[19] S. Abbas, M.A. Saleem, S.M.S. Kazmi, M.J. Munir, Production of sustainable clay bricks using waste fly ash: mechanical and durability properties, J. Build. Eng. 14 (2017) 7–14, https://doi.org/10.1016/j.jobe.2017.09.008.

[20] M. Sutcu, H. Alptekin, E. Erdogmus, Y. Er, O. Gencel, Characteristics of fired clay bricks with waste marble powder addition as building materials, Construct. Build. Mater. 82 (2015) 1–8, https://doi.org/10.1016/j.conbuildmat.2015.02.055.

[21] M. Sutcu, J.J. del Coz Díaz, F.P. Álvarez Rabanal, O. Gencel, S. Akkurt, Thermal performance optimization of hollow clay bricks made up of paper waste, Energy Build. 75 (2014) 96–108, https://doi.org/10.1016/j.enbuild.2014.02.006.

[22] B. Angjusheva, V. Ducman, E. Fidanchevski, The effect of the addition of construction & demolition waste on the properties of clay-based ceramics, Sci. Sinter. 54 (2022) 359–371.

[23] S.M.S. Kazmi, S. Abbas, M.A. Saleem, M.J. Munir, A. Khitab, Manufacturing of sustainable clay bricks: utilization of waste sugarcane bagasse and rice husk ashes, Construct. Build. Mater. 120 (2016) 29–41, https://doi.org/10.1016/j.conbuildmat.2016.05.084.

[24] A.M. Rasool, A. Hameed, M.U. Qureshi, Y.E. Ibrahim, A.U. Qazi, A. Sumair, Experimental study on strength and endurance performance of burnt clay bricks incorporating marble waste, J. Asian Architect. Build Eng. 22 (2023) 240–255, https://doi.org/10.1080/13467581.2021.2024203.

[25] K.L. Lin, Feasibility study of using brick made from municipal solid waste incinerator fly ash slag, J. Hazard Mater. 137 (2006) 1810–1816, https://doi.org/10.1016/j.jhazmat.2006.05.027.

[26] O. Kizinievič, V. Voišnienė, V. Kizinievič, I. Pundienė, Impact of municipal solid waste incineration bottom ash on the properties and frost resistance of clay bricks, J. Mater. Cycles Waste Manag. 24 (2022) 237–249, https://doi.org/10.1007/s10163-021-01314-4.

[27] B. Angjusheva, E. Fidancevska, V. Ducman, Influence of the main process parameters on the physical and mechanical properties of the bottom ash ceramics, Quality. Life (banja luka) - Apeiron 14 (2016), https://doi.org/10.7251/QOL1603059A.

[28] P.N. Lemougna, J. Yliniemi, H. Nguyen, E. Adesanya, P. Tanskanen, P. Kinnunen, J. Roning, M. Illikainen, Utilisation of glass wool waste and mine tailings in high performance building ceramics, J. Build. Eng. 31 (2020) 101383.

[29] P.N. Lemougna, J. Yliniemi, A. Ismailov, E. Levanen, P. Tanskanen, P. Kinnunen, J. Roning, M. Illikainen, Recycling lithium mine tailings in the production of low temperature (700–900 °C) ceramics: effect of ladle slag and sodium compounds on the processing and final properties, Construct. Build. Mater. 221 (2019) 332–344, https://doi.org/10.1016/j.conbuildmat.2019.06.078.

[30] B. Sena da Fonseca, C. Galhano, D. Seixas, Technical feasibility of reusing coal combustion by-products from a thermoelectric power plant in the manufacture of fired clay bricks, Appl. Clay Sci. 104 (2015) 189–195, https://doi.org/10.1016/j.clay.2014.11.030.

[31] SFS-EN 12457-2, Characterisation of waste, Leaching. Compliance test for leaching of granular waste materials and sludges. One Stage Batch Test at a Liquid to Solid Ratio of 10 L/kg for Materials with Particle Size below 4 Mm (Without or with Size Reduction), 2002.

[32] ASTM C 666/C 666M – 03, Standard Test Method for Resistance of Concrete to Rapid Freezing and Thawing, 2008.
[33] A. Adediran, P.N. Lemougna, J. Yliniemi, P. Tanskanen, P. Kinnunen, J. Roning, M. Illikainen, Recycling glass wool as a fluxing agent in the production of clay-and waste-based ceramics, J. Clean. Prod. 289 (2021) 125673.
[34] S. Wang, L. Gainey, I.D.R. Mackinnon, Y. Xi, High- and low-defect kaolinite for brick making: comparisons of technological properties, phase evolution and microstructure, Construct. Build. Mater. 366 (2023) 130250, https://doi.org/10.1016/j.conbuildmat.2022.130250.
[35] D. Suescum-Morales, R.V. Silva, M. Bravo, J.R. Jiménez, J.M. Fernández-Rodríguez, J. de Brito, Effect of incorporating municipal solid waste incinerated bottom ash in alkali-activated fly ash concrete subjected to accelerated CO2 curing, J. Clean. Prod. 370 (2022) 133533, https://doi.org/10.1016/j.jclepro.2022.133533.
[36] A. Adediran, J. Yliniemi, S. Moukannaa, D.D. Ramteke, P. Perumal, M. Illikainen, Enhancing the thermal stability of alkali-activated Fe-rich fayalite slag-based mortars by incorporating ladle and blast furnace slags: physical, mechanical and structural changes, Cement Concr. Res. 166 (2023) 107098, https://doi.org/10.1016/j.cemconres.2023.107098.
[37] P.N. Lemougna, A. Ismailov, E. Levanen, P. Tanskanen, J. Yliniemi, K. Kilpimaa, M. Illikainen, Upcycling glass wool and spodumene tailings in building ceramics from kaolinitic and illitic clay, J. Build. Eng. 81 (2024) 108122, https://doi.org/10.1016/j.jobe.2023.108122.
[38] E.H. Dagnew, Alternative resource of incineration bottom ash for ceramic tile production, Internat. J. Ceramic Eng. Sci. 4 (2022) 281–285, https://doi.org/10.1002/ces2.10136.
[39] ASTM C62, ASTM C62-23, Standard Specification for Building Brick (Solid Masonry Units Made from Clay or Shale), 2023.
[40] S. Wang, L. Gainey, I.D.R. Mackinnon, C. Allen, Y. Gu, Y. Xi, Thermal behaviors of clay minerals as key components and additives for fired brick properties: a review, J. Build. Eng. 66 (2023) 105802, https://doi.org/10.1016/j.jobe.2022.105802.
[41] S. Guzlena, G. Sakale, S. Certoks, L. Grase, Sand size particle amount influence on the full brick quality and technical properties, Construct. Build. Mater. 220 (2019) 102–109, https://doi.org/10.1016/j.conbuildmat.2019.05.170.
[42] R. Taurino, E. Karamanova, L. Barbieri, S. Atanasova-Vladimirova, F. Andreola, A. Karamanov, New fired bricks based on municipal solid waste incinerator bottom ash, Waste Manag. Res. 35 (2017) 1055–1063, https://doi.org/10.1177/0734242X17721343.
[43] S. Potrč, M. Bogataj, Z. Kravanja, Z.N. Pintarič, 6th international conference on technologies & business models for circular economy: conference proceedings, univerzitetna založba univerze v mariboru. https://doi.org/10.18690/um.fkkt.1.2024, 2024.
[44] I. Netinger Grubeša, M. Vračević, V. Ducman, B. Marković, I. Szenti, Á. Kukovecz, Influence of the size and type of pores on brick resistance to freeze-thaw cycles, Materials 13 (2020) 3717, https://doi.org/10.3390/ma13173717.
[45] A. Adediran, J. Yliniemi, V. Carvelli, E. Adesanya, M. Illikainen, Durability of alkali-activated Fe-rich fayalite slag-based mortars subjected to different environmental conditions, Cement Concr. Res. 162 (2022) 106984, https://doi.org/10.1016/j.cemconres.2022.106984.
[46] P.N. Lemougna, J. Yliniemi, E. Adesanya, P. Tanskanen, P. Kinnunen, J. Roning, M. Illikainen, Reuse of copper slag in high-strength building ceramics containing spodumene tailings as fluxing agent, Miner. Eng. 155 (2020) 106448, https://doi.org/10.1016/j.mineng.2020.106448.
[47] S. Ferrari, A.F. Gualtieri, The use of illitic clays in the production of stoneware tile ceramics, Appl. Clay Sci. 32 (2006) 73–81, https://doi.org/10.1016/j.clay.2005.10.001.
[48] I. Pitak, A. Baltušnikas, R. Kalpokaitė-Dičkuvienė, R. Kriukiene, G. Denafas, Experimental study effect of bottom ash and temperature of firing on the properties, microstructure and pore size distribution of clay bricks: a Lithuania point of view, Case Stud. Constr. Mater. 17 (2022) e01230, https://doi.org/10.1016/j.cscm.2022.e01230.
[49] D. Eliche-Quesada, J. Leite-Costa, Use of bottom ash from olive pomace combustion in the production of eco-friendly fired clay bricks, Waste Manag. 48 (2016) 323–333, https://doi.org/10.1016/j.wasman.2015.11.042.
[50] M. Sutcu, E. Erdogmus, O. Gencel, A. Gholampour, E. Atan, T. Ozbakkaloglu, Recycling of bottom ash and fly ash wastes in eco-friendly clay brick production, J. Clean. Prod. 233 (2019) 753–764, https://doi.org/10.1016/j.jclepro.2019.06.017.
[51] G. El Boukili, M. Ouakarrouch, M. Lechheb, F. Kifani-Sahban, A. Khaldoune, Recycling of olive pomace bottom ash (by-Product of the clay brick industry) for manufacturing sustainable fired clay bricks, Silicon 14 (2022) 4849–4863, https://doi.org/10.1007/s12633-021-01279-x.